

## Property of Novel Sodium Ion Exchanger $\text{Li}_{1.4}\text{Cr}_{0.2}\text{Al}_{0.2}\text{Ti}_{1.6}(\text{PO}_4)_3$

JIAN-ZHI SUN

*Department of Chemistry Dezhou University, Dezhou 253023, China.*

(Received on 28<sup>th</sup> June 2008, accepted in revised form 22<sup>nd</sup> March 2010)

**Summary:** A novel sodium specific kind of ion exchanger  $\text{Li}_{1.4}\text{Cr}_{0.2}\text{Al}_{0.2}\text{Ti}_{1.6}(\text{PO}_4)_3$  fabricated by a solid-state reaction method. The microstructure XRD, FTIR, Raman spectra, adsorption performances were investigated. The average grain size of the samples was about 70–90  $\mu\text{m}$ . FTIR and Raman spectra studies were carried out and the vibrational bands were assigned. XRD analysis showed that the structure of  $\text{Li}_{1.4}\text{Cr}_{0.2}\text{Al}_{0.2}\text{Ti}_{1.6}(\text{PO}_4)_3$  convert to  $\text{Na}_{1.4}\text{Cr}_{0.2}\text{Al}_{0.2}\text{Ti}_{1.6}(\text{PO}_4)_3$  after adsorption. The exchange capacity reaches 34.12 mg/g, under adsorption duration 12 h, temperature 50 °C. The experimental results showed that the Na/Li ion exchange reaction rate increased obviously for  $\text{Li}_{1.4}\text{Cr}_{0.2}\text{Al}_{0.2}\text{Ti}_{1.6}(\text{PO}_4)_3$  with increasing temperature, and the Na/Li ion exchange kinetics process of  $\text{Li}_{1.4}\text{Cr}_{0.2}\text{Al}_{0.2}\text{Ti}_{1.6}(\text{PO}_4)_3$  in lithium chloride solution could be represented approximately by the equation of JMAK.

### Introduction

Salt lake resources are very abundant in China and lithium in the brine is very famous in the world, but now, the exploitation of salt lake resources in China is just at the elementary and single-use level. At present, the demands for lithium chloride, especially the highly pure lithium chloride, are increasing rapidly. Lithium chloride is an industrial raw material, from which lithium compounds and in particular metallic lithium are produced. To make processing of the lithium chloride more economic and efficient, it is very necessary to provide the raw material as pure as possible. The presence of very small quantities of sodium in the lithium metal will make it highly reactive and much different in properties than pure lithium metal. So the raw material LiCl is required with low Na content.

The ordinary Li separation method is to extract sodium with isopropanol, which not only consumes substantive organic solvent, but also is serious harm to environment. The adsorption method is brief and feasible in theory, but the synthesis of an applicable adsorbent is a big problem. Antimonic and polyantimonic acid have been studied in the field but it failed in practice because of high cost [1]. At present, to meet the rapidly increasing demand on lithium chloride, specially high by pure lithium chloride, it is urgent to remove  $\text{Na}^+$  to produce high pure lithium chloride.

NASICON (Acronym of natrium superionic conductor) materials present interesting sensitive and

selective properties against alkaline cations due to their structure.  $\text{Li}_{1+x}\text{Al}_x\text{Ti}_{2-x}(\text{PO}_4)_3$  possesses the NASICON-type structure, is especially good candidate to determine alkaline ions concentrations in solution or to separate monovalent cations from a mixture of multivalent ions [2, 3].

$\text{Li}_{1+x}\text{Al}_x\text{Ti}_{2-x}(\text{PO}_4)_3$  composed of both  $\text{MO}_6$  octahedra and  $\text{PO}_4$  tetrahedra which are linked by their corners to form an opened-three-dimension (3D) network structure. The resulted structure consists of Type I sites (octahedral O-coordination) and Type II sites (10-fold O-coordination) for the mobile Li ions to occupy.  $\text{Li}^+$  ions move from one site to another passing through bottle-necks defined by the anionic skeleton  $[\text{Al}_x\text{Ti}_{2-x}(\text{PO}_4)_3]^{(1-x)-}$  [2].

Chromium and aluminum have similar valence and chemical properties. Chromium are widely used in the field of functional materials and new material [4]. Therefore, an attempt was made to improve the adsorption performance by substituting Cr for Al.

The results indicated that  $\text{Li}_{1.4}\text{Cr}_{0.2}\text{Al}_{0.2}\text{Ti}_{1.6}(\text{PO}_4)_3$  (LCATP) show higher exchange capacities towards  $\text{Na}^+$ . The exchange capacity of LCATP was 34.12 mg/g. Compared with other methods, the novel Na specific ion exchanger of LCATP described here is a simple and more convenient way to remove  $\text{Na}^+$  from LiCl solution which suggest the promising application.

## Results and Discussion

Fig. 1 shows TG-DTA curves of the raw material. There are two endothermic peaks at 128.2 °C, 193.6 °C in TG-DTA curves. TG curve revealed the mass loss of 29.37% which occurred at 150 °C to 600 °C, while no change in weight was found from 600~1000 °C. The following reaction can be expected to have mass loss of 29.58%:

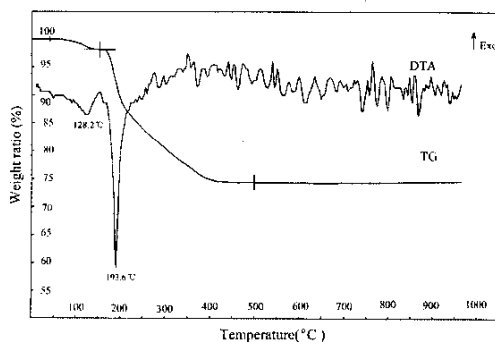
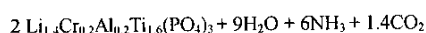
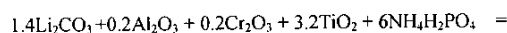


Fig. 1: TG-DTA curves of the raw material.

The phase evolution of diffraction patterns LCATP were studied by the XRD analysis (Fig. 2). The substitution of Cr for Al was tried synthetically to observe the change of the crystalline structure. The LCATP structure was same to  $\text{LiTi}_2(\text{PO}_4)_3$ . It was indexed in the rhombohedral system with lattice: rhomb-centered, space group R3c and the cell parameters:  $a = 0.8518\text{ nm}$ ,  $b = 0.8518\text{ nm}$ ,  $c = 2.087\text{ nm}$ ,  $\alpha = 90^\circ$ ,  $\beta = 90^\circ$ ,  $\gamma = 120^\circ$ .

The ion exchange mechanism is further supported by the XRD contrast of the adsorbent before and after adsorbing. Continuous shifts of the diffraction peaks towards smaller values of  $2\theta$  are observed. The ion exchange of  $\text{Na}^+/\text{Li}^+$  enhance lattice constants, which was ruling factor leading to the shifts of the diffraction peaks. The ionic exchange reaction is:

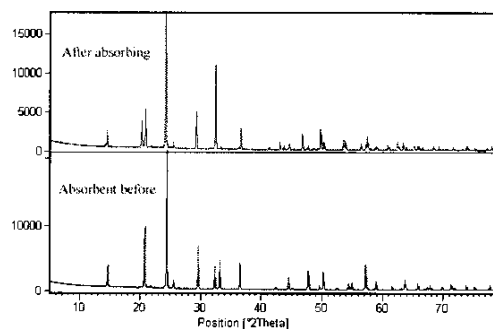
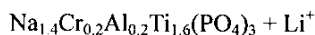
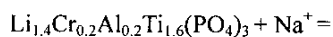


Fig. 2: XRD contrast of the adsorbent before and after adsorbing.

Fig. 3 showed microstructure of the fracture surfaces of the specimen pellet heat-treated at 1000 °C. It was seen that the specimen are highly dispersive particles with diameters ranged at 70~90  $\mu\text{m}$ .

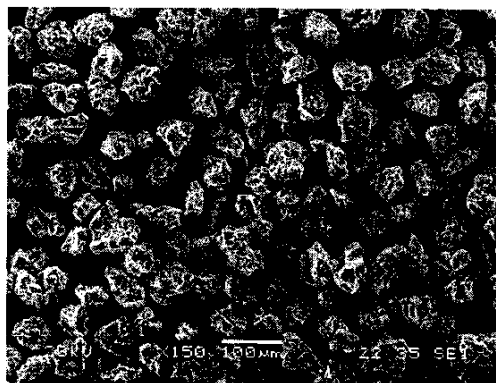


Fig. 3: Scanning electron microscope (SEM) photograph of LCATP.

Infrared absorption spectra of LCATP are presented in Fig. 4. The spectra are dominated by intense, overlapping intramolecular  $\text{PO}_4^{3-}$  stretching modes that range from 1300 to 700  $\text{cm}^{-1}$ . The frequency of the broad features between 700 and 850  $\text{cm}^{-1}$  in the spectrum of LCATP are somewhat lower than expected for  $\text{PO}_4^{3-}$  stretching modes. In fact, bands in this region of the spectrum are often due to condensed phosphate groups such as  $\text{P}_2\text{O}_7^{4-}$  or extended polyphosphate structures. However, there are no bands near 750  $\text{cm}^{-1}$  in the infrared spectrum to indicate the presence of bridging P-O-P groups. Raman spectroscopy is particularly useful in

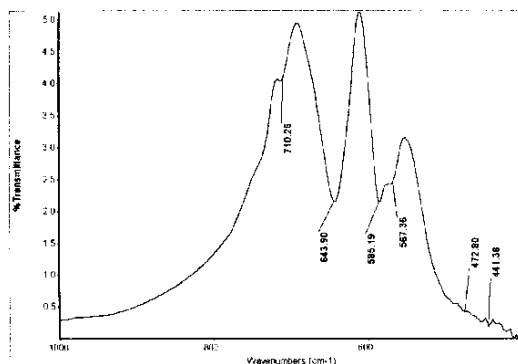


Fig. 4: Fourier transform infrared (FTIR) spectra of  $\text{Li}_{1.4}\text{Cr}_{0.2}\text{Al}_{0.2}\text{Ti}_{1.6}(\text{PO}_4)_3$ .

identifying condensed phosphates as the P–O–P bending motions (across the bridging oxygen atom) yield intense bands between  $700$  and  $800\text{ cm}^{-1}$  in the Raman spectrum. The lack of any spectral activity in this region strongly argues that the LCATP sample does not contain a significant fraction of condensed phosphate groups [5, 6].

In LCATP,  $\nu_4$  is expected to yield five IR active vibrational modes at the Brillouin zone center ( $2A_{2u}+3E_u$ ), and two IR active modes are expected for  $\nu_2$  ( $2E_u$ ). Four bands detected at  $710.26$ ,  $643.90$ ,  $585.19$  and  $567.36\text{ cm}^{-1}$  of LCATP are assigned to  $\nu_4$ . The far-IR spectrum of LCATP contains at least two intense bands at  $472.80$  and  $441.38\text{ cm}^{-1}$ . The  $\nu_2$  vibrations probably occur within this spectral range, however, it is difficult to assign these modes with confidence because some of the external modes are also expected to occur at these frequencies [7].

Raman scattering spectra of the intramolecular  $\text{PO}_4^{3-}$  stretching modes ( $\nu_1$  and  $\nu_4$ ) of LCATP are presented in Fig. 5. The spectrum of LCATP is dominated by three intense bands at  $1008.561$ ,  $993.133$  and  $978\text{ cm}^{-1}$  and a weaker band at  $1097.272\text{ cm}^{-1}$ . Group theory predicts  $\nu_1$  will yield two Raman active modes ( $A_{1g}+E_g$ ), whereas  $\nu_3$  will give six Raman active vibrations ( $A_{1g}+2A_{2g}+3E_g$ ) at the Brillouin zone center for LCATP. The vibrational modes are classified according to the irreducible representations of the  $D_{3d}$  point group, which is isomorphic to the factor group. It is tempting to assign the two bands at  $993.133$  and  $978\text{ cm}^{-1}$  to  $\nu_1$  and the bands at  $1097.272$ ,  $1070.273$  and  $1008.561$

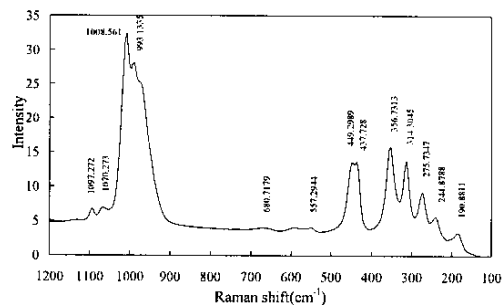


Fig. 5: Raman scattering spectra of LCATP.

$\text{cm}^{-1}$  to  $\nu_3$  since the  $\text{PO}_4^{3-}$  symmetric stretching modes typically occur at lower frequencies than the asymmetric modes [7].

The asymmetric bending modes ( $\nu_4$ ) are assigned to the very weak bands above  $500\text{ cm}^{-1}$ , while the bands at  $449.299$  and  $437.728\text{ cm}^{-1}$  are thought to consist mostly of symmetric bending motions ( $\nu_2$ ). The larger intensities of  $\nu_2$  bands compared to  $\nu_4$  are due to the highly symmetrical  $\text{PO}_4^{3-}$  anions in LCATP, further supporting the assignment of the strong Raman band at  $1008.561\text{ cm}^{-1}$  to predominately  $\nu_1$  vibrations. External modes occur below  $360\text{ cm}^{-1}$  in the Raman spectra of LCATP. In general, it is extremely difficult to assign bands in this region of the spectrum because the modes are highly mixed, consisting of a mixture of different types of atomic motion. The bands at  $275.7347\text{ cm}^{-1}$  are assigned to translational vibrations of the  $\text{Ti}^{4+}$  ions, while the bands at  $314.3045$ ,  $244.8788$ ,  $190.8811\text{ cm}^{-1}$  are assigned to modes that predominantly contain  $\text{PO}_4^{3-}$  motions [7].

As shown in Fig. 6 the amount of  $\text{Na}^+$  exchange capacity increases with contact time and attains equilibrium within 12 h for ion exchanger at  $50$  and  $80^\circ\text{C}$ .

The higher temperature is good for ion exchange. The diffuse rate of  $\text{Li}^+$  and  $\text{Na}^+$  increase in  $\text{LiCl}$  solution, LCATP and  $\text{Na}_{1.4}\text{Cr}_{0.2}\text{Al}_{0.2}\text{Ti}_{1.6}(\text{PO}_4)_3$ , which accelerates  $\text{Na/Li}$  ion exchange on LCATP.

Kinetics law of  $\text{Na/Li}$  ion exchange fraction on LCATP depended on time can be express using JMAK equation [8].

$$x = 1 - e^{-kt^n} \quad (1)$$

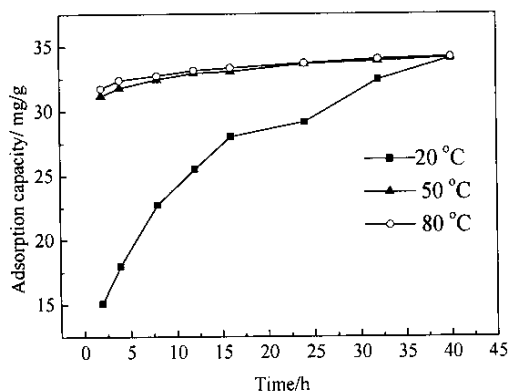


Fig. 6: Influence of temperature on exchange capacity.

where  $x$ , ion exchange fraction of Na/Li on LCATP at  $t$  time;  $K$ , empirical parameter which is affected by temperature and granularity;  $n$ , time gene.

The equation may be linearized by taking the logarithm of both sides of eq. (1) and linear form of JMAK equation can be given as eq. (2):

$$\ln[-\ln(1-x)] = n \ln t + \ln K \quad (2)$$

The constant values of the isotherms were obtained from the slope and intercept of the plots (Fig. 7). The JMAK equation represents adequately the Kinetics law of  $\text{Na}^+$  on LCATP.

### Experimental

#### Preparation of $\text{Li}_{1.4}\text{Cr}_{0.2}\text{Al}_{0.2}\text{Ti}_{1.6}(\text{PO}_4)_3$

$\text{Li}_{1.4}\text{Cr}_{0.2}\text{Al}_{0.2}\text{Ti}_{1.6}(\text{PO}_4)_3$  was prepared by solid state reaction of  $\text{Li}_2\text{CO}_3$  (A. R.),  $\text{TiO}_2$  (A.R.),  $\text{Al}_2\text{O}_3$  (A.R.),  $\text{Cr}_2\text{O}_3$  (A.R.),  $\text{NH}_4\text{H}_2\text{PO}_4$  (A.R.),  $\text{C}_6\text{H}_{14}$  (A.R.). The starting materials were weighed in stoichiometric amounts and homogenized using a mixer. The mixture was put in a tubular furnace and had been heated for 6 h at  $600^\circ\text{C}$  to decompose the oxalate and the phosphate. The powder was cooled down to room temperature and then pressed into  $\Phi$  10 mm pellets under 20 MPa. After again grinding and homogenization, the mixture was transferred to the furnace and annealed at  $1000^\circ\text{C}$  for 20 h.

TG-TGA was carried out by employing a TA SDT Q600. The samples were heated to  $1000^\circ\text{C}$  at a heating rate of  $10^\circ\text{C}/\text{min}$  under nitrogen atmosphere.

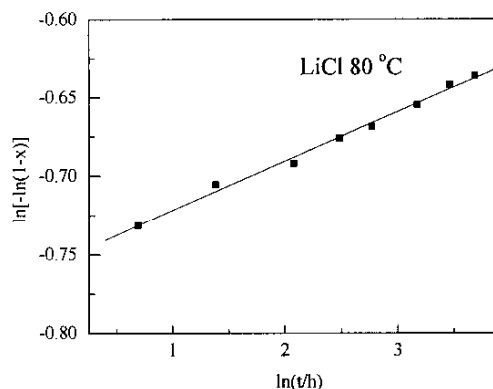
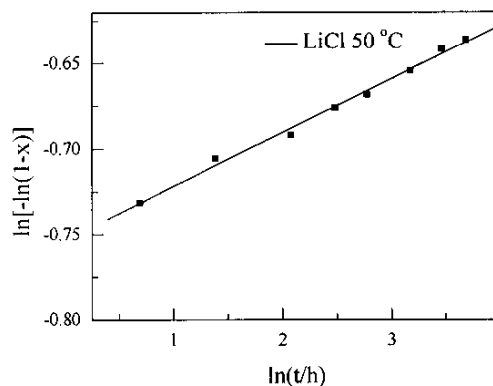
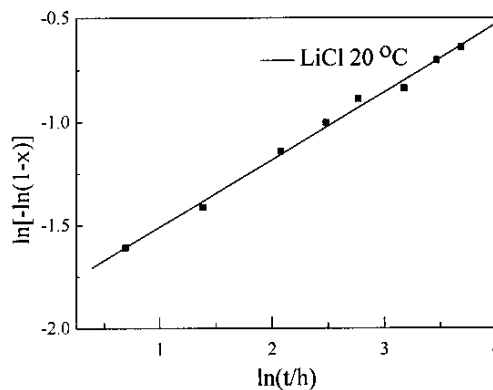


Fig. 7:  $\ln[-\ln(1-x)]$  against  $\ln t$  of Na/Li ion-exchange of LCATP.

XRD was performed at room temperature on a Rigaku D/max-3B X-Ray diffractometer, the X-ray beam was nickel-filtered  $\text{Cu } K\alpha$  ( $\lambda = 0.15406 \text{ nm}$ ) radiation operated at 40 kV and 30 mA; and the data were collected from  $3^\circ$  to  $80^\circ$  ( $2\theta$ ) at a scanning rate of  $5^\circ/\text{min}$ .

FTIR spectra were recorded on a Thermo Nicolet Nexus. Care was taken to press all the KBr

pellets under the same conditions to minimize any effect of pressure on peak frequencies for the samples.

#### *Measurements of adsorption capacity*

1.0 g diffraction patterns of LCATP samples were added to 100 g LiCl solution contained 0.06% Na<sup>+</sup>. The concentration of Na<sup>+</sup> in solution is measured after stirring the solution for 12 h. The ion exchange capacity of LCATP samples was carried out at different temperature.

#### **Conclusions**

A novel sodium specific kind of ion exchanger LCATP has been successfully prepared. The specimen treated at 1000 °C for 12 h displayed the high exchange capacity. Moreover, solid-state reaction method has been demonstrated as a simple and useful procedure to prepare LCATP. The exchange capacity reaches 34.12 mg/g, under adsorption duration 12 h, temperature 50 °C. XRD analysis showed that the structure of Li<sub>1.4</sub>Cr<sub>0.2</sub>Al<sub>0.2</sub>Ti<sub>1.6</sub>(PO<sub>4</sub>)<sub>3</sub> convert to Na<sub>1.4</sub>Cr<sub>0.2</sub>Al<sub>0.2</sub>Ti<sub>1.6</sub>(PO<sub>4</sub>)<sub>3</sub> after adsorption. The JMAK equation represents adequately the Kinetics law of Na<sup>+</sup> on LCATP.

#### **Acknowledgments**

This work was supported by the grant from the Technology Research and Development Program of Dezhou(No. 20080153) and the Foundation of dezhou University human resources(No. 07rc003).

#### **References**

1. Deberitz, Jurgen, Kobele, Klaus, Schade. *U S Patent 6,063,345*, 2000.
2. E. R. Losilla, and M. A. G. Aranda, *Chemistry of Materials*, **12**, 2134 (2000).
3. A. Puigsegur, and R. Mouazer, *Separation and Purification Technology*, **32**, 51 (2003).
4. M. Barre, F. Le Berre, and M. P. Crosnier-Lopez, *Chemistry Material*. **18**, 5486 (2006).
5. M. Javid, *Journal of the Chemical Society of Pakistan*, **28**, 323 (2006).
6. M. Christopher, Burba, and R. Frech, *Solid State Ionics*, **177**, 1489 (2006).
7. Jingwei Xu, and F. R. Denis, *Spectrochimica Acta Part A.*, **54**, 1869 (1998).
8. L. Tai-Ping, and W. Jia-Liang, *Acta Physics-Chemistry Sinica*, **23**, 1642 (2007).